ρ^* SCALING EXPERIMENTS FOR ELMY H-MODES IN JET

B. Balet, D. Campbell, J.P. Christiansen, J.G. Cordey, C. Gormezano, C. Gowers, D. Muir, E. Righi, G.R. Saibene, P.M. Stubberfield.
JET Joint Undertaking, Abingdon, Oxfordshire, OX14 3EA

1. Introduction

L-mode scaling experiments have been made on TFTR, JET in which all dimensionless parameters describing the plasma, its geometry, the magnetic field, are held constant; only the normalised Larmor radius $\rho*$ is varied. The scaling of local and global confinement in such experiments is found to be the Bohm scaling and corresponds to a local one fluid diffusivity

$$\chi = \chi_B \, \rho_*^{x_\rho} \, F\left(\nu_*, \beta, q_\psi, \varepsilon, \ldots\right), \quad x_\rho = 0 \tag{1}$$

in the Connor-Taylor representation; $\chi_B = T/B$ is the Bohm diffusivity and the unknown function F of the dimensionless parameters $\nu*$, β, ... is held constant in the experiments. The result (1) is compatible with the global scaling law ITER89P. The values of the arguments of F on JET are those foreseen for ITER, only

$$\rho_*^{ITER} = \frac{1}{4} \rho_*^{JET} \tag{2}$$

Extrapolation from JET to ITER using the result (1) yields $\tau_\varepsilon \approx 1.5$s which is too short for achieving ignition in an L-mode plasma. It is thus necessary to explore other operating regimes like H-modes with or without ELMs. The scaling of confinement with ρ_* in ELMy H-modes has recently been reported by DIIID [1]. The experimental conditions were chosen to match a particular scenario developed by the ITER team. A single-null X-point plasma configuration characterised by the parameter values given in Table I has been used on both DIIID and JET. The recent JET experiments include both scans in ρ_* as well as power threshold scans at various densities and fields. In both the DIIID and JET experiments NBI (D into D) is applied. The safety factor q_ψ at the 95% radius has been either 3.4 or 3.7 (see Table I) on JET and 3.7 on DIIID.

2. Similarity below, and above the L to H Transition

We first examine some consequences from the confinement scaling laws as regards similarity in dimensionless variables. The magnetic field, temperature, density and total energy can be expressed in terms of dimensionless variables and one dimensional variable which we choose as minor radius a. Thus

$$B \sim a^{-5/4}\,\rho_*^{-3/2}\,\nu_*^{-1/4}\,\beta^{1/4} \quad , \quad n \sim a^{-2}\,\rho_*^{-2}\,\nu_*^{0}\quad \beta \tag{3}$$

$$T \sim a^{-1/2}\,\rho_*^{-1}\quad \nu_*^{-1/2}\,\beta^{1/2} \quad , \quad W \sim a^{1/2}\,\rho_*^{-3}\,\nu_*^{-1/2}\;\beta^{3/4} \tag{4}$$

The power required to achieve an energy W is

$$P \sim a^{-3/4}\rho_*^{-5/2+x_\rho}\,\nu_*^{-3/4}\,\beta^{7/4}\,F(\nu_*, \beta, \ldots) \tag{5}$$

For power levels well below the threshold power needed to establish an H-mode [2] we would expect the ITER89P L-mode scaling law [3] to apply; at the L→H transition the threshold power law may apply [2]: for power levels well above the threshold, the ITER93H Elm-free or ELMy scaling laws [4] should apply. We therefore insert the specific scalings of F from [2-4] to derive power scalings with respect to a, ρ_*, ν_*, β

$$P_{ITER89P} \quad \sim \quad a^{-3/4}\;\rho_*^{-5/2}\;\nu_*^{-1/2}\;\beta^{2} \tag{6a}$$

$$P_{THR} \quad \sim \quad a^{-3/4}\;\rho_*^{-3}\;\nu_*^{-1/2}\;\beta^{3/2} \tag{6b}$$

$$P_{ITER93H} \quad \sim \quad a^{-3/4}\;\rho_*^{-3/2}\;\nu_*^{-0.65}\;\beta^{3} \tag{6c}$$

The variations with ρ_* are known as respectively: Bohm (6a), Goldston (6b), gyro-Bohm (6c) scalings. From (6a-c) we see that at fixed ν_*, β these 3 lines in ($P_a^{3/4}$, ρ_*) space will intersect. As a consequence when $\rho_* \rightarrow 0$ the selected β for the H-mode may be below the threshold required to establish an H-mode.

3. Results

Data from 28 pulses has been examined. In (ν_*, β, q_{95}) space the relevant data during the ELMy phase occupies a volume exceeding by far that given by the data ranges in Table I. One reason for this is the variability of ELM-type, amplitude and frequency. It is however possible to isolate pairs of discharges with an acceptable degree of similarity during the ELMy H-mode phase. Table I contains data values for 2 such pairs of pulses with $q_\psi = 3.4$ and 3.7 respectively. The values (non-steady) of P_{loss} and P_{THR} are time averages during the ELMy phase.

The first pair of pulses (#33131, #33140) exhibits a power dependence on ρ_* close to the Goldston, i.e. the threshold scaling Eq. (6b) with $x_\rho = -0.5$ in Eq. (1). In contrast it can be seen that the second set (#35156, #35171) show a much weaker power dependence on ρ_* close to the gyro-Bohm scaling Eq. (6c) with $x_\rho = +1$ in Eq. (1).

A local transport analysis with the TRANSP code has been carried out for the 4 pulses in Table I. The procedures for cross-checking the various sources of data

for consistency have been applied as described in [5]. The spatially varying density and temperature profiles are reasonably well matched as described by Eqs. (3,4). In these high density ELMy H-modes the density profiles are almost constant across the discharge unlike the T_e profiles with a centre-edge ratio of 4. To demonstrate the consistency between global and local data we evaluate profiles of the effective diffusivity χ_{eff} of a one-fluid description. According to Eq. (1) the ratios of χ_{eff} profiles should equal the ratios of $\rho_*^{x_p}$. Figure 1 shows the radial dependence of the χ_{eff} ratio for the second set of pulses. The dotted lines refer to ratios expected from $x_\rho = 1$ (gyro-Bohm), $x_\rho = 0$ (Bohm), $x_\rho = -1$ (Stochastic) and correspond to respectively $\chi \sim B^{-1}$, $B^{-1/3}$ and $B^{+1/3}$. Figure 1 shows ratios corresponding to the gyro-Bohm scaling for these two pulses just as Table I predicts this dependence upon total power.

4. Discussion

The different ρ_* dependencies seen in the two sets of pulses of Table I can be attributed to various effects:

1. The types of ELMs produced in the 4 pulses differ and consequently so do the periods in which the discharges revert from H to L and then back to H mode confinement.

2. Many theories predict the H-mode threshold as well as "a confinement barrier" to depend upon edge parameters only and not core parameters as used here.

The results obtained emphasise that the gyro-Bohm scaling does not hold close to the threshold. We emphasise this point in Figure 2 which shows normalised power "$Pa^{3/4}$" versus ρ_*^{-3} (i.e. Eq. 6b). In Fig. 2 the DIIID points originate from [1].

This has the following implication for ITER: an extrapolation from JET to ITER in ρ_* at constant ν_*, β, q using gyro-Bohm scaling can only be made if the ITER data point, i.e. the ITER power level, considerably exceeds the level predicted by the threshold scaling.

Table I

Pulse	B [T]	ρ_* [10^{-4}]	β_{th}	ν_* [10]$^{-3}$	q_{95}	P_{LOSS} [MW]	P_{THR} [MW]
33131	3	1.9	0.6	7	3.7	19.6	9.95
33140	1.7	2.7	0.6	7	3.7	6.3	3.51
35156	2	2.05	0.7	8	3.4	9.1	5.48
35171	1	3.6	0.7	8	3.4	4.8	1.77

References

[1] Petty, C, et al., in Physics of Plasmas, Vol. 2 2342 (1995).

[2] Ryter, F., et al., Controlled Fusion and Plasma Physics, Proceedings of 21st Conference, Montpellier I (1994) 334.

[3] Yushmanov, P.N., et al., Nucl. Fusion 30 (1990) 1999.

[4] Thomsen, K, et al.., Nucl. Fusion 34 (1994) 131.

[5] Balet, B., et al., Nucl. Fusion 32 (1992) 1261.

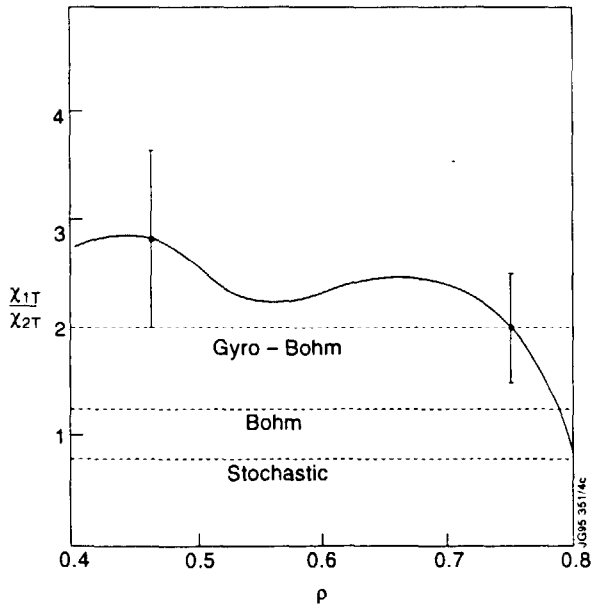

Fig. 1. The ratio of the effective thermal diffusivities versus the normalised radial co-ordinate $\rho(\sim r/a)$. The dashed lines are the expected ratio for gyro-Bohm, Bohm and stochastic scalings.

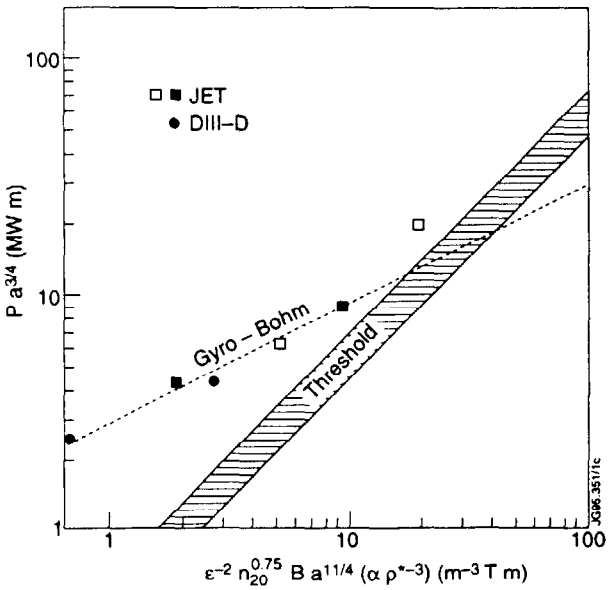

Fig. 2. Normalised power $Pa^{3/4}$ versus ε^{-2} $n^{0.75}$ $Ba^{11/4}$ $(\alpha\ \rho^{*-3})$, the open squares are #33131 and #33140 and the solid squares #35156, #35171. The hatched area is one of the threshold expressions in reference (2), the DIII-D points are from Petty et al[1].